The EMBO Journal Vol. 21 No. 22 pp. 6036–6049, 2002

Cell numbers and leaf development in *Arabidopsis*: a functional analysis of the *STRUWWELPETER* gene

Daphné Autran, Claudia Jonak[1], Katia Belcram, Gerrit T.S.Beemster[2], Jocelyne Kronenberger, Olivier Grandjean, Dirk Inzé[2] and Jan Traas[3]

Laboratoire de Biologie Cellulaire, INRA, Route de Saint-Cyr, 78026 Versailles cedex, France, [1]Institute of Microbiology and Genetics, Vienna Biocenter, University of Vienna, Dr Bohrgasse 9, 1030 Vienna, Austria and [2]Department of Plant Systems Biology, Vlaams Interuniversitair Instituut voor Biotechnologie, Universiteit Gent, K.L. Ledeganckstraat 35, B-9000 Gent, Belgium

[3]Corresponding author
e-mail: Jan.Traas@versailles.inra.fr

D.Autran and C.Jonak contributed equally to this work

The *struwwelpeter* (*swp*) mutant in *Arabidopsis* shows reduced cell numbers in all aerial organs. In certain cases, this defect is partially compensated by an increase in final cell size. Although the mutation does not affect cell cycle duration in the young primordia, it does influence the window of cell proliferation, as cell number is reduced during the very early stages of primordium initiation and a precocious arrest of cell proliferation occurs. In addition, the mutation also perturbs the shoot apical meristem (SAM), which becomes gradually disorganized. *SWP* encodes a protein with similarities to subunits of the Mediator complex, required for RNA polymerase II recruitment at target promoters in response to specific activators. To gain further insight into its function, we overexpressed the gene under the control of a constitutive promoter. This interfered again with the moment of cell cycle arrest in the young leaf. Our results suggest that the levels of SWP, besides their role in pattern formation at the meristem, play an important role in defining the duration of cell proliferation.

Keywords: leaf development/Mediator complex/primordia/shoot apical meristem

Introduction

In multicellular animals and plants, body size is often correlated with cell number, and it has been suggested that the strict control of cell division is an important factor in the regulation of growth and development (Raff, 1996; Conlon and Raff, 1999; Vernoux *et al*., 2000c). However, other views exist, based on cases where substantial alterations in cell proliferation do not alter organ size or developmental patterns. In imaginal wing discs of *Drosophila*, for example, the overexpression of E2F, a transcription factor promoting cell division, leads to increased cell number, but the final wing size remains normal as the cells are smaller. Conversely, overexpression of the *Drosophila* homologue of the retinoblastoma protein reduces cell numbers, but again wing size is not affected (reviewed in Day and Lawrence, 2000; Weinkove and Leevers, 2000). Similar observations have been made for plants. Tobacco expressing a dominant-negative version of the *Arabidopsis* cell cycle regulator CDKA (cdc2aAt) showed almost normally sized leaves with fewer and larger cells (Hemerly *et al*., 1995). More recently, overexpression of inhibitors of cell division, the so-called KIP-related proteins (KRPs), reduced cell numbers in *Arabidopsis* leaves, a defect that was largely compensated by increased cell size (Wang *et al*., 2000; De Veylder *et al*., 2001). Together, these observations suggest that intrinsic mechanisms exist, operating throughout the organ or organism as a unit and dictating size and shape. According to such a scenario, cell proliferation or expansion itself would not be strictly regulated in time and space by a complex network of instructions given to the individual cells, but would simply follow growth patterns coordinated at the tissue level (Kaplan and Hagemann, 1991; Potter and Xu, 2001). The molecular basis underlying such a concept, however, is unclear. In addition, conflicting data exist. For example, overexpression of E2Fa and Dpa, two transcription factors involved in the activation of cell cycle genes, induces extra cell divisions in *Arabidopsis* plants, but also severely inhibits overall growth of the plant (De Veylder *et al*., 2002). This would suggest that overall growth of the organs does depend on the proliferative status of the individual cells. Therefore, the importance of cells as a level of developmental control remains a matter of debate (Kaplan and Hagemann, 1991; Vernoux *et al*., 2000c; Potter and Xu, 2001; Traas and Doonan, 2001).

To investigate the regulation and functional significance of cell proliferation in plants, we have taken a genetic approach. For this purpose, we have started to analyse a set of mutants with abnormal cell division patterns and cell numbers. Here we present a recessive mutant, *struwwelpeter* (*swp*), which shows perturbed meristem function and dwarfism. The reduced organ size is due to a substantial reduction of cell number in all aerial organs. Although, in some organs, this defect is partially compensated by an increase in final cell size, final organ size is usually severely reduced. We present evidence that the mutation affects the mechanisms that control cell number during primordium initiation and the timing of cell cycle arrest later on in development. The *SWP* gene encodes a protein with similarities to metazoan and yeast Med150/*RGR1*-like subunits of the Mediator transcriptional regulatory complex of RNA polymerase II activity. Experiments involving overexpression studies further suggest that the leaf cell number depends on the level of *SWP* expression.

Results

General phenotype of the swp mutant

During a screen of T-DNA mutagenized lines for mutants perturbed in meristem function and organ initiation (Bechtold *et al*., 1993), we found a recessive mutant

with reduced leaf number and leaf size. This mutant was named *swp*. Because *swp* homozygotes are sterile, the mutation was propagated via heterozygous plants.

The mutant develops as a dwarf (Figure 1A–D) with an abnormal architecture, including stem fasciation and abnormal floral structure. Root structure was normal, and root growth was only slightly reduced (data not shown). Until 6 days after sowing, seedlings were indistinguishable from the wild type, implying that embryonic development was not markedly disrupted. After 6 days, however, the *swp* phenotype became apparent as the cotyledons were slightly lanceolated and a somewhat darker green. Subsequently, the outgrowth of the first leaf pair was retarded. The leaves produced in *swp* mutants were small and showed aberrant morphologies with reduced blade expansion. Due to the reduced leaf blade, the boundaries between lamina and petiole were macroscopically not very distinct (Figure 1A and D). Leaf shapes were variable from one individual to another at the same stage (Figure 1A), ranging from almost radial symmetrical finger-shaped leaves to more developed blades, which often displayed asymmetrical serrations. Moreover, the first leaves were often more dramatically affected, suggesting that the requirement for *SWP* varied during shoot development. Since the phenotype became apparent during the development of the first leaves, we next concentrated on mutant leaves to study cellular aspects.

Cell numbers and cell size in mature leaves of the swp mutant

To test whether the reduced leaf size observed in *swp* mutants was correlated with a reduction in cell size and/or in cell number, the adaxial lamina surface of the first two expanded leaves was visualized using scanning electron microscopy (SEM), 28 days after sowing in soil. The *Arabidopsis* wild-type leaf epidermis contains three cell types: pavement cells with highly convoluted cell walls resulting in a jigsaw-puzzle-like pattern, stomata and trichomes. Although the size of the pavement cells is highly variable in *Arabidopsis* (Van Lijsebettens and Clarke, 1998), comparison of the *swp* and wild-type epidermal pavement cells revealed an increase in cell size in the mutant (Figure 1E and F). This was quantified through SEM images of three mature leaves of each genotype grown in the greenhouse. The results showed a significant increase (Student's *t*-test, $p < 0.005$) of the mean cell size of ~30% in the mutant (10 200 μm^2, 100 cells measured) when compared with the wild type (6680 μm^2, 101 cells measured). This increase also concerned the stomata (mean surface of individual guard cells, 280 μm^2 in wild type and 396 μm^2 in the mutant). Trichomes were normal in size and sometimes even showed reduced branching (data not shown). In addition, a similar defect was observed in the inner leaf tissues (data not shown). We concluded that the smaller leaf size was due to a reduction in the number of cells per leaf. This reduction was partially compensated by an increase in final cell size.

swp was similar to certain mutants perturbed in adaxial/abaxial polarity, which show small, narrow lateral organs. To analyse the effect on polarity, we examined the position of trichomes on the first leaves and the distribution of spongy and palisade mesophyll. In the wild type, juvenile leaves only show trichomes on the adaxial side. This was also the case for *swp* mutants, even in very lanceolated leaves (data not shown). Similarly, we did not find an abnormal organization of the mesophyll; in plastic sections of both mutant and wild-type leaves, palisade mesophyll was found on the adaxial side. Since there was no obvious defect in organ polarity, we did not investigate this aspect further.

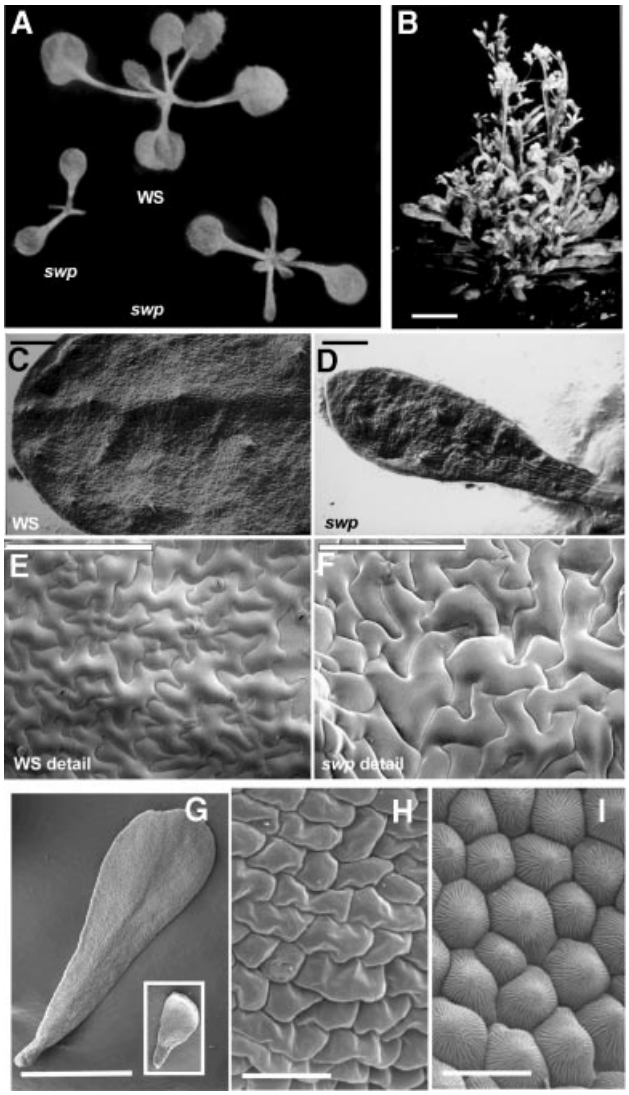

Fig. 1. General plant phenotype and mature leaves in *swp* mutant. (**A**) Sixteen-day-old wild-type and *swp* plants grown *in vitro*. (**B**) *swp* mature plant grown in soil. Mature first rosette leaves of 4-week-old wild-type (**C** and **E**) and *swp* (**D** and **F**) plants were visualized using SEM. Although *swp* leaves displayed a severely reduced size (D) compared with wild-type ones (C, same magnification as in D), adaxial epidermal cells are larger (compare E with F, same magnification), showing that cell number is reduced in *swp* (F). (**G–I**) Petal size and cell size. Mutant petals inset in G are much smaller than wild-type petals (G). This difference in overall size is not compensated by extra cell expansion, as the cells in the mutant petal (H) are even somewhat smaller than those in the wild type (I). Scale bars: 1.5 mm (B); 1 mm (C and D); 200 μm (E and F); 500 μm (G); 20 μm (H and I).

Cell numbers and cell size in other organs

To define the effects of the mutation on other organs, we next examined stems, flowers and floral organs in the SEM. Although these organs showed an important vari-

ability in size and shape, the observations confirmed that cell numbers were reduced throughout development. This reduction was quantified in petals using the same method as for the kinematic analysis (see below). This showed that the number of epidermal cells on the adaxial side of the petals was reduced from 5700 in the wild type (SE 302.55; 24 petals) to 1800 in the mutant (SE 175.42; 24 petals).

Interestingly, the reduced cell number was not compensated by an increase in cell size in all organs (Figure 1G–I). Whereas in sepals, cells tended to be bigger, the cells in the petals tended to be even smaller, resulting in a greatly reduced size of the mutant petals. We therefore concluded that the *swp* mutation causes a reduction in cell number throughout development, but that compensatory mechanisms leading to extra cell growth were limited to certain organs only.

Cell proliferation rates in swp

How is the reduction in cell number achieved during *swp* leaf development? We first tested the possibility that the mutation directly perturbs the cell cycle machinery by prolonging the duration of the cell cycle. In turn, this could lead to a reduced number of cell cycles during the proliferative phase of the leaf cells, as described for the KRP overexpressers (De Veylder *et al*., 2001). We therefore measured this parameter *in vivo*, using confocal microscopy and a vital plasma membrane dye. For this purpose, 93 and 62 dividing epidermal cells of plantlets grown *in vitro* were followed for five wild-type and five *swp* primordia, respectively. Reconstructions of serial sections taken every 12 h, from 6 to 8 days after sowing, were analysed (Figure 2A and B). A large majority of these cells in both the wild type and mutants had divided during the first 24 h of the experiment (88 and 87% in wild-type and mutant leaves, respectively). After 36 h, approximately half of the cells had undergone a second or even third division (52% of the cells in wild type and 63% of the cells in mutant primordia; Figure 2C). The similar duration of the cell cycle in mutant and wild type was confirmed by measurements of the mitotic index on fixed material (data not shown). Together, these data indicated that the differences in cell numbers in the mutant leaves compared with wild-type leaves were due to problems arising during the start and/or arrest of cell divisions in the developing leaves. To obtain more information on the evolution of cell division over time, we used the kinematic analysis described by De Veylder *et al*. (2001).

Start and arrest of cell proliferation during leaf development

Leaves of mutant and wild-type plants grown *in vitro* were harvested at daily intervals between 6 and 20 days after sowing, i.e. from the stage when the mutant could be recognized onwards. Subsequently, leaf area and average cell area were determined. From these data, the average cell number per leaf was calculated. The abaxial epidermis was used in this study because it lacks trichomes. At 6 days after sowing, a reduction of ~40% in leaf area was already observed in the mutant. This difference increased until it reached ~10-fold reduction (Figure 3A). As stated previously, the reduction of *swp* leaf area (Figure 3A) is not due to a reduction in cell size (Figure 3B) but to a decrease in cell number (Figure 3C), already evident from the

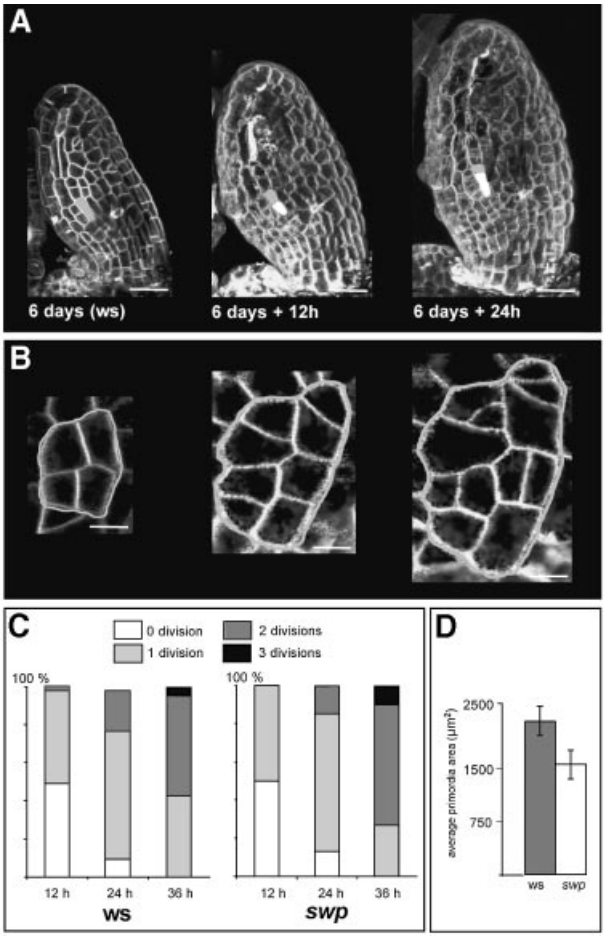

Fig. 2. *In vivo* analysis of cell proliferation in *swp* leaf primordia and organ size in early *swp* primordia. (**A**) Epidermal cell divisions were followed by analysing reconstructions of serial sections of living primordia, made every 12 h. (**B**) Detail showing divisions undergone within 36 h by a group of four epidermis cells. (**C**) The rate of cell proliferation in wild-type and *swp* primordia was evaluated by scoring the number of cells that had divided zero times, one time, two times or three times, 12, 24 and 36 h after the start of the experiment, at 6 days after sowing. (**D**) The mean primordia area measured on median longitudinal sections in 2-day-old wild-type and *swp* seedlings is significantly different between *swp* and wild-type (Student's *t*-test, $p < 0.05$). Scale bars: 40 µm (A); 5 µm (B).

earliest stages observed in this experiment. In 20-day-old *swp* plants, ~10-fold fewer cells were present than in wild-type leaves (Figure 3C). As indicated above, this reduction was partially compensated by an increase in final cell size when plants were grown in soil. Interestingly, this compensation did not occur *in vitro*. When plants were grown in Petri dishes, the mutant leaves were clearly smaller than the wild-type leaves, but the final cell size was very comparable (Figure 3B). Therefore, the differences in leaf area from plants grown *in vitro* were directly proportional to the decrease in cell numbers.

Relative cell division rate was determined by calculating the slope of the exponential log 2 cell number curves (Figure 3D). Note that this is different from the absolute cell division rate in individual cells. The calculated cell division rate also depends on the number of cells no longer actively dividing in the primordium. In wild-type plants, the relative cell division rates rapidly declined between 8 and 14 days after sowing. Lower rates were maintained thereafter. Until 8 days after sowing, the relative cell

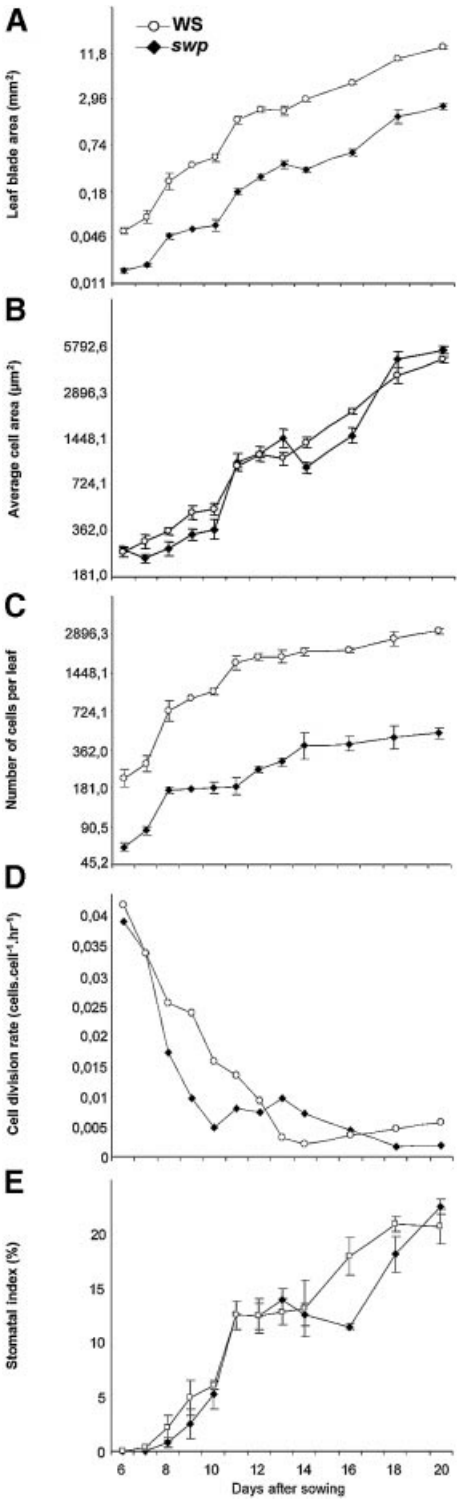

Fig. 3. Kinematic analysis of *swp* leaf development. Kinematic analysis was performed on the first leaf pair of wild-type (WS) (open circles) and *swp* plants (black diamonds). Cells of abaxial epidermis were analysed. (**A**) Average leaf blade area. (**B**) Average cell area. (**C**) Average number of cells. (**D**) Cell division rate. (**E**) Stomatal index.

division rate in *swp* and wild-type plants was comparable. From day 8 until day 12, however, the values were significantly lower in *swp*. This indicated that, in the mutant, a significant proportion of the cells had stopped dividing. Average cell cycle duration in the whole leaf can be estimated as the inverse of the relative cell division rate. At day 8, when most of the cells in both genotypes were still proliferating, the average cell cycle durations were 25.8 and 25.6 h in wild-type and *swp* primordia, respectively.

This global kinematic analysis of leaf development not only confirmed that the maximal proliferation rates in the young primordia were comparable, but also suggested that in *swp* leaves, a majority of epidermal cells stopped dividing earlier than in wild-type plants. However, the reduction in cell number observed in mature *swp* leaves was not merely the result of a precocious arrest in cell division, since *swp* leaves had a reduced cell number very early in development. At 6 days after sowing, the mutant leaves already showed a 2- to 4-fold reduction in cell number. This, in turn, suggested that *swp* primordia could already have reduced cell numbers at the moment the primordium anlagen are formed. To test this hypothesis, we examined primordium size at the time of germination.

swp homozygotes are sterile and seedlings homozygous for the *swp* mutation are macroscopically indistinguishable from wild-type seedlings before 6 days after sowing. To test whether a reduction in primordium size existed in the *swp* mutant at earlier stages, we took advantage of the non-invasive confocal microscopy technique to visualize 4-day-old living primordia in the progeny of a *swp* heterozygous plant. The young seedlings were then returned to the growth chamber until 9 days after sowing, when the *swp* leaf phenotype could be unambiguously detected. In this way, we could trace back the early phenotype of 30 *swp* primordia and compare them with 54 wild-type primordia. The mean area of median sections through the 4-day-old mutant primordia was 1628 μm^2, which represented a 28% reduction when compared with the wild type (2273 μm^2; Figure 2D). Since cell size in the mutant was similar to the wild type during the early phases of leaf development (Figure 3B), these observations favoured a model in which the primordia anlagen themselves contained reduced cell numbers.

The timing of cell differentiation in swp

Does the early arrest of cell division cause early cell differentiation in *swp* mutant? To address this question, we looked at this process in the leaves. We first determined the evolution of the stomatal index, which was used previously by De Veylder *et al*. (2001). This parameter was similar in *swp* and wild-type leaves (Figure 3E), indicating that cell differentiation proceeded normally. Indeed, SEM images of the mature *swp* leaf surface (Figure 1C–F) and confocal microscopy of fixed and living *swp* primordia showed that differentiation of other morphological markers such as trichomes, or the establishment of vascular tissue, was normal in *swp*. Later on in development, however, cell differentiation could be perturbed. Mutant petals, for example, did not show the typical ridges on their cellular surfaces usually observed in the wild type (Figure 1G–I).

We next investigated another early marker of differentiation, i.e. endoreduplication. In *Arabidopsis* leaf epidermal cells, the arrest of cell division is followed by the onset of endocycles, leading to increased cell DNA content, and correlated with cell expansion (Traas *et al*., 1998). The ploidy levels of *swp* and wild-type mature first leaves were measured 4 weeks after sowing in soil. In wild-type leaves,

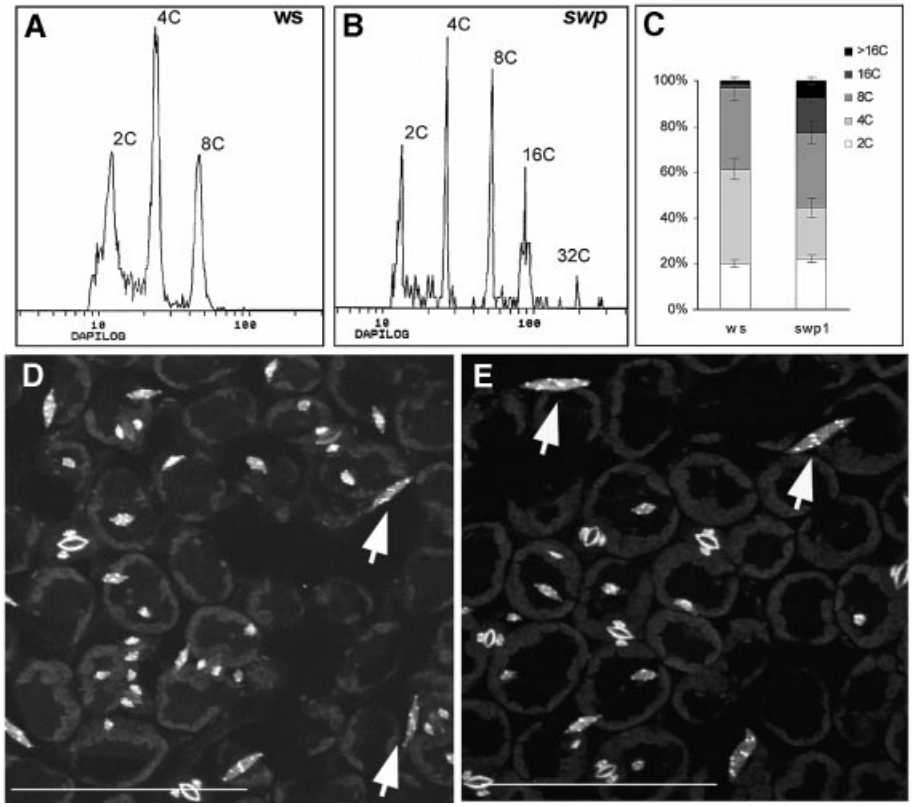

Fig. 4. Ploidy level measurements in mature *swp* leaves. Cell flow cytometric profiles of wild-type (**A**) and *swp* (**B**) leaves of 4-week-old plants. Quantification of ploidy distribution is represented (**C**) as mean ± SD of three independent measurements involving different sets of plants. (**D**) and (**E**) show a projection of several confocal sections through the epidermis of full-grown wild-type (D) and mutant (E) leaves stained for DNA with propidium iodide. Note that the spindle-form nuclei of the pavement cells (arrows) are bigger in the mutant. The nuclei of stomata have the same size. Bars: 125 μm.

cells presenting a DNA content of 2C, 4C and 8C were detected (Figure 4A and C). In *swp* leaves, 2C, 4C and 8C cells were present; however, ~20% of the nuclei analysed presented a 16C DNA content, reducing the proportion of 4C and 8C cells as compared with wild-type leaves (Figure 4B and C). A small 32C peak could even be detected. This showed that in *swp* leaves, a significant proportion of the cells went through one or even two additional rounds of endoreduplication after the arrest of mitosis. To determine whether a specific population of cells was concerned with the extra endoreduplication, we stained the leaves for DNA, before visualization in the fluorescence microscope. This revealed that a majority of the pavement cells and some of the mesophyll cells contained larger nuclei, not observed in the wild type, and contained more DNA (Figure 4D and E).

Effects of the swp mutation on shoot apical meristem (SAM) maintenance

Apart from leaf size and shape, shoot development showed a range of other abnormalities in *swp* mutants. In 16-day-old *swp* seedlings, the rosette leaf number was reduced (2.2 leaves per plant ± 1.7) compared with the wild type (5.5 leaves per plant ± 1.5) (Figure 1A). In addition, the mutants showed perturbed phyllotaxis throughout development; *swp* mutants always displayed a significant delay in flowering, leading to the formation of a rosette with many leaves (Figure 1B). The stems initiated were often fasciated, with short internodes and multiple cauline leaves. The flowers usually showed an abnormal architecture, with abnormal organ numbers. This highly pleiotropic shoot phenotype clearly suggested severe defects in shoot apical meristem function. We therefore analysed the effects of the mutation on SAM organization.

To detect potential early defects in SAM structure at 6 days, 42 wild type and 49 mutants were examined using conventional sectioning or confocal microscopy. This revealed no significant structural perturbations of the mutant SAM, which was indistinguishable from the wild type (Figure 5A). At later stages, however, SAM organization was progressively disrupted in *swp*. In longitudinal sections of 13-day-old wild-type seedlings, the wild-type SAM presented a characteristic dome-shaped structure (Figure 5B). In contrast, the *swp* SAM at this stage was flat, with only a few layers of meristematic cells, which appeared as small, densely stained cells. These layers were irregular, with more vacuolated cells present in the centre of the inner layers. The anticlinal planes of cell division, which characterize the L1 and L2 layers in wild-type SAM, were merely visible in a single outer cell layer in *swp* (Figure 5C). As the mutants developed, these perturbations increased: in the 20-day-old *swp* SAM, the organization into layers was clearly altered. The enlarged SAM surface showed groups of meristematic-type cells adjacent to large vacuolated ones developing in an aberrant structure (Figure 5D and E).

These results suggested that a progressive loss of organization occurred into the *swp* SAM after germin-

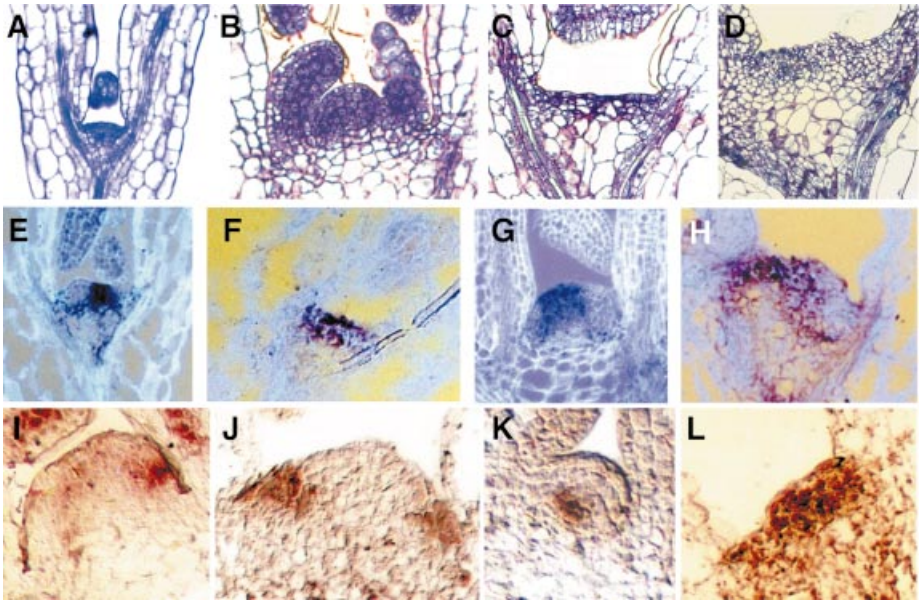

Fig. 5. Shoot apical meristem organization and maintenance in the *swp* mutant. (**A**–**D**) Histological sections of meristems stained with toluidine blue. In 6-day-old seedlings in the progeny of *swp* heterozygous plants, the SAM structure is indistinguishable from the wild type [(A) representative of the 60 individual plants examined]. Thirteen-day-old wild-type seedlings present a characteristic dome-shaped SAM (B). In contrast, the *swp* SAM at this stage is flat, with only a few irregular meristematic cell layers (C). The 20-day-old *swp* SAM region is enlarged and shows groups of vacuolated cells adjacent to meristematic type cells (D). (**E**–**H**) STM expression pattern in wild-type (E and G) and *swp* (F and H) meristems. From 8 days after germination onward (F), STM expression in *swp* becomes irregular. This situation increased in 16-day-old plants (H). Note that downregulation of STM at the level of the incipient leaf primordia is systematically observed in *swp*. (**I** and **J**) ANT expression in wild-type (I) and *swp* (J) primordia anlagen. (**K** and **L**) WUS expression pattern. In 10-day-old wild-type SAM, WUS is expressed in a central group of inner cells of the SAM (K). In *swp* SAM at the same stage, WUS is ectopically expressed in an irregular pattern across the SAM (L).

ation. To obtain further insight into the functional organization of the *swp* SAM, the identity of the cells within the apex was examined by analysing the expression patterns of meristem markers using *in situ* hybridization. *SHOOTMERISTEMLESS* (*STM*) is a homeobox gene required for meristem formation and maintenance. In wild-type plants, this gene is expressed by all cells in the SAM. It is downregulated as the cells are recruited in the organ anlagen, at the flanks of the meristem (Long *et al*., 1996; Figure 5E and G). The expression pattern was different in *swp*. In 8-day-old mutants, some cells in the internal layers of the SAM failed to express *STM* (Figure 5F) resulting in an irregular expression pattern. Sixteen days after germination, *STM* is expressed in groups of cells across the *swp* apex, separated by cells that do not express the gene (Figure 5H). This results in a patchy pattern. Cells in this region continued to divide, resulting in the formation of a callus-like tissue in some of the plants. At the level of the young primordia, downregulation of *STM* and upregulation of the primordium marker *AINTEGUMENTA* (*ANT*) was systematically observed (Figure 5H–J), suggesting that primordia cells were able to differentiate normally. Thus, consistent with the previous histological observations, these data show that cells in the *swp* SAM progressively lose meristematic identity as judged by the failure to maintain the integrity of the *STM* expression domain.

Since there was a clear defect in meristem maintenance, we next examined the *WUSCHEL* (*WUS*) gene, which is involved in meristem stem cell fate maintenance and is expressed in a group of central cells underneath the three outermost layers in the wild-type SAM (Mayer *et al*., 1998; Figure 5K). In 8-day-old *swp* mutants, patches of cells expressing *WUS* are visible in central as well as peripheral regions and in the outer layers of the SAM (Figure 5L). Thus, the localization of *WUS* expression is disrupted in *swp*. Indeed, *WUS* is ectopically expressed in an irregular pattern across the *swp* SAM.

Cloning of the SWP gene

To gain further insight in *SWP* function, the cloning of the gene was undertaken. The *swp* mutant allele was identified in the Versailles T-DNA mutant collection. Plants heterozygous for the *swp* mutation were backcrossed twice to Wassilewskija (WS) wild-type plants. Subsequently, 1301 *swp* mutant seedlings were transferred to kanamycin-containing medium. All of these were kanamycin resistant, indicating a tight linkage between the kanamycin resistance locus of the T-DNA and the *swp* mutation. Southern blot analysis of the mutant DNA using probes corresponding to the T-DNA revealed a single insertion (data not shown). DNA fragments flanking both sides of the T-DNA were subsequently cloned by inverse PCR and plasmid rescue, and used to screen an *Arabidopsis* genomic DNA library. Sequencing of several overlapping positive genomic clones and comparison with current databases showed that the cloned fragments were identical to a region of BAC F7O18 at the top of chromosome 3. The T-DNA is inserted at the 5′ end of a gene encoding a hypothetical protein (Figure 6A) and ~3 kb downstream of the ATG of the early auxin-induced gene IAA16 (Kim *et al*., 1997) situated in an inverse orientation relative to the previous gene. A wild-type genomic IAA16 clone did not rescue, even partially, the *swp* mutation (data not shown), indicating that this gene is not affected by the *swp* mutation. However, insertion of

the T-DNA had a significant effect on the transcription of the neighbouring gene (see below), which was thus a good candidate for *SWP*.

We identified a truncated EST (H10G5T7) corresponding to the 3′ end of the gene. A complete cDNA sequence was isolated by 5′ RACE PCR. Comparison of the cDNA with the genomic sequence showed that the gene contains six introns and seven exons (Figure 6A). The T-DNA flanking sequences isolated from the *swp* mutant indicated that the T-DNA was inserted 250 bp 5′ of the start codon, close to the predicted transcription start site of the gene. This cDNA has the potential to encode a protein of 1703 amino acids (aa).

Similarity of SWP to Med150/RGR1-like subunits of Mediator transcriptional regulatory complex

Analysis of the predicted 1703 aa *SWP* protein sequence indicated that it encodes a hydrophobic protein of 186 kDa, which contains two putative nuclear localization signals (Raikhel, 1992). A serine-rich region (aa 645–767) was also detected in the predicted protein sequence (complete protein sequence under DDBJ/EMBL/GenBank accession No. AJ511271).

The *SWP* protein sequence was compared with known proteins in databases using the BLAST program (Altschul *et al*., 1997). The N-terminal domain of *SWP* showed significant sequence similarity to a series of large proteins homologous to the *Saccharomyces cerevisiae* cMed150/RGR1 protein, a component of the RNA polymerase II Mediator complex (Figure 6E; Li *et al*., 1995; accession No. P19263). Within this domain, *SWP* showed 51% similarity (aa 39–284) to the 1454 aa human hMed150/TRAP170 protein (Gu *et al*., 1999). The 1521 aa *Drosophila* gene product dMed150/dTRAP170 (accession No. AE003468) displayed 43% similarity to *SWP* in the N-terminal domain (aa 39–483). In addition, a short domain of stronger similarities (62%) was detected in the C-terminal parts of the two proteins (aa 1476–1524 of the *SWP* sequence, Figure 6F). Significant similarities were also detected to the N-terminal part of a homologous hypothetical protein from *Caenorhabditis elegans.* When compared with one another, all these proteins display similar N-terminal domains. Moreover, their overall sizes are similar (Figure 6E). A comparison with the complete *Arabidopsis* genome revealed that *SWP* encodes a unique protein.

Complementation of the swp mutant

To confirm that we had identified the *SWP* gene, a wild-type genomic sequence encompassing the *SWP* candidate gene (Figure 6A) was cloned into a plant transformation vector containing hygromycin resistance and used to transform kanamycin-resistant plants heterozygous for the *swp* mutation. All 310 hygromycin- and kanamycin-resistant primary transformants (T1) displayed a wild-type phenotype at the seedling level (cotyledon shape, initiation of the first leaf pair; Figure 6B). Twenty-two of these T1

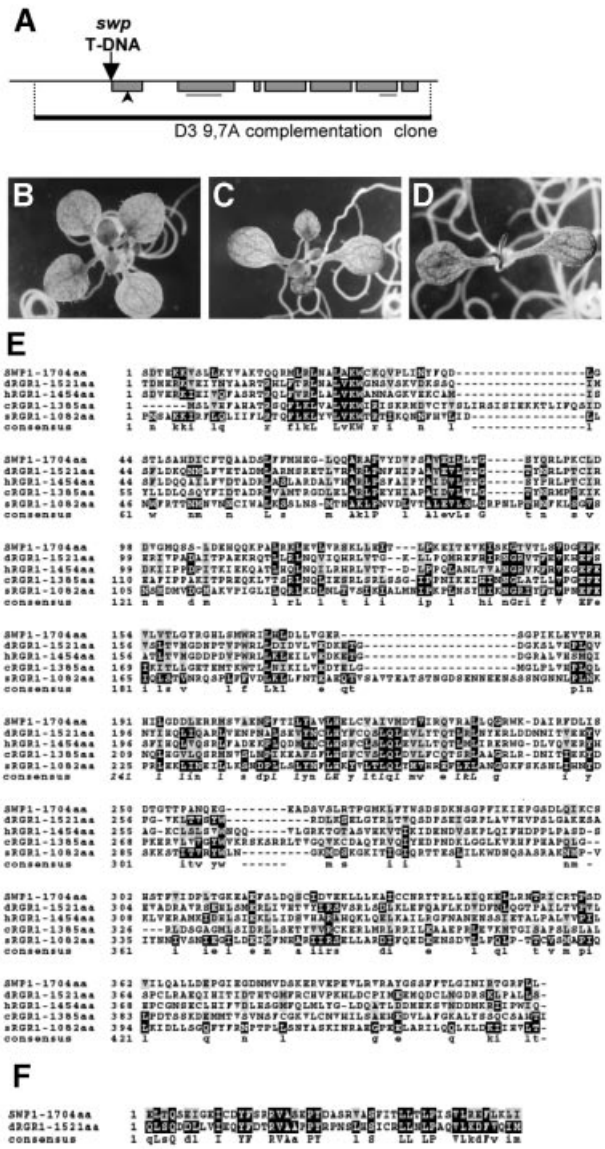

Fig. 6. The *SWP* gene: gene structure, phenotypic restoration and similarity to Med150/RGR1-like proteins. (**A**) The *SWP* gene (*SWP1*) contains six introns (lines) and seven exons (boxes). The SWP cDNA has the potential to encode a 1703 aa polypeptide from the initiating methionine (arrowhead) situated 250 bp downstream of the 5′end of the cDNA. Also shown is the position of the T-DNA insertion in the swp1 mutant line. A 1.3 kb promoter region has been shown to be sufficient to drive SWP expression in phenotypic restoration experiments (see text) using the D3-9.7 genomic clone that is represented. The two regions of the SWP1 putative protein showing significant similarity to Med150/RGR1-like proteins are shown (light grey bars). (**B–D**) Fourteen-day-old seedlings *in vitro* grown from *swp* homozygote plants containing a transgenic copy of the SWP gene (D3-9.7 genomic clone represented above) and exhibiting a wild-type phenotype (B, line 8) or a partially restored phenotype (C, line 23), as compared with non-transgenic *swp* seedlings segregating in the same line (line 8, D). (**E**) The N-terminal domain of SWP protein (SWP; F7018.23 protein; AAF04900.1; residues 39–442) was aligned with similar regions (N-terminal domains) of the human hMed150/TRAP170/hRGR1/DRIP150/EXLM1 protein (hRGR1; gb AAD24360.1; residues 77–327), *Drosophila* dMed150/dTRAP170/RGR1 protein (dRGR1; AAG02462 GadFly identifier: CG12031; residues 63–466), mouse mRGR1 protein (mRGR1; dbj BAA76610.1; residues 83–333), putative *C.elegans* 157 kDa protein C38C10.5 (cRGR1; pir S28289; residues 1–264) and yeast (*S.cerevisae*) sMed150/RGR1 protein (RGR1; dbj BAA14104.1; residues 123–286). The number of amino acids for the full proteins is indicated. (**F**) A C-terminal domain of SWP (residues 1232–1335) was aligned with a conserved domain of the *Drosophila* protein dRGR1 (residues 1418–1524, C-terminal position). All alignments were performed using the Clustal_W and Boxeshade softwares at Infobiogen (http://www.infobiogen.fr/services/analyses).

plants were transferred to soil. Mature plants were all normal and fertile. Analysis of the T2 progeny revealed that 11 of the transferred T1 plants were homozygous for kanamycin resistance, and thus for the *swp* mutation, and heterozygous for hygromycin resistance. As expected for such a genotype, all T2 offspring (943 observed seedlings) were kanamycin resistant, while a quarter were composed of hygromycin-sensitive mutant seedlings (mean values are 31.5 hygromycin sensitive versus 149.1 resistant plants). The remaining 50% of the T1 plants were heterozygous for both resistance markers. This demonstrated that even a single copy of the construct employed was able to restore a wild-type phenotype. This result showed that we had identified the *SWP* gene and confirmed that *swp* is a loss of function mutation.

In addition, a partial phenotypic restoration, probably due to a weaker expression level of the transgene, was observed in one of the complemented lines (Figure 6C). In that case, hygromycin-resistant seedlings sometimes displayed the dark and narrow cotyledon shape typical of homozygous *swp* seedlings. Leaf development, however, was less altered in these plants (Figure 6, compare C with D). Although the first leaves were small and lanceolated, the following leaves were gradually less affected. Flowering time was also delayed and stem development was affected in such plants, but to a lesser extent than in the *swp* mutant (data not shown).

Consequences of T-DNA insertion on SWP expression in the swp mutant

The expression of the *SWP* gene was first examined in wild type and the *swp* mutant by RNA blot analysis. In wild-type plants, a single band of ~5.5 kb was observed, consistent with the expected size of the mRNA. In contrast, in *swp* mutant plants, a band of ~7 kb was visible, together with several smaller bands embedded in smears, probably indicating that mRNA degradation had occurred. Moreover, the 7 kb mutant transcript was significantly more abundant than the 5.5 kb transcript of the wild type (Figure 7A). Because the T-DNA (carrying the 35S CaMV promoter next to the left border) is inserted close to the predicted transcription start site in the *swp* line, it is possible that the initiation of transcription is impaired.

To test whether the larger transcript in the mutant was due to a fusion between *SWP* and T-DNA sequences, RT–PCR was performed, using primers for the left border of the T-DNA and the 5′ end of the *SWP* cDNA. A fragment could be amplified from *swp* RNA and not from the wild-type control RNA (Figure 7B). This result indicated that *swp* produced chimeric mRNAs composed of the left border of the T-DNA fused to the *SWP* mRNA. This chimeric mRNA may be under control of the 35S promoter.

SWP mRNA expression pattern

The expression pattern of *SWP* during development was analysed using RNA *in situ* hybridization (Figure 8). During embryogenesis, *SWP* mRNA was detected in all cells, from the early octant to the cotyledonar stage (Figure 8B, torpedo stage). This is very different from *STM* mRNA, which is only present in the SAM of the embryo (Figure 8A), used here as a positive control. After

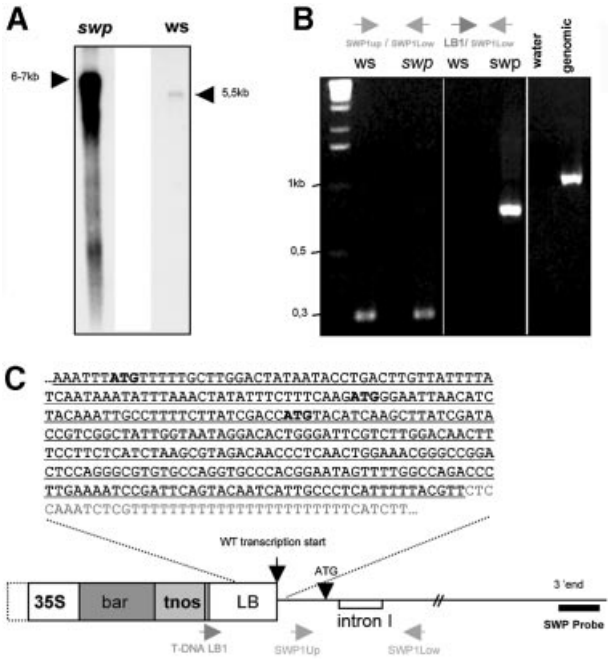

Fig. 7. Consequences of T-DNA insertion on *SWP* expression in *swp* mutant. (**A**) Northern blot analysis of *SWP* expression in the *swp* mutant showing overproduction of aberrant transcripts in swp. A northern blot with ~2 μg of poly(A)+ RNA from *swp* homozygote plants (*swp*) or wild-type plants (ws) was hybridized with a *SWP* RNA-specific probe corresponding to the 3′ end of the cDNA (represented in C). RNA size was estimated using a RNA ladder run on the same gel. (**B**) RT–PCR experiment showing fusion of *SWP* mRNA with T-DNA left border region in *swp* mutant. Total RNA from *swp* plants (*swp*) or wild-type plants (ws) were reverse transcribed and amplified using primers designed to the 5′ end of the *SWP* cDNA (swpUp) and to the T-DNA left border (LB1) (represented in C). A 0.7 kb fragment could be amplified from *swp* RNA (lane 4) and not from WS RNA (lane 3). Amplification using primers from the *SWP* cDNA only (swpUp/swpLow; see C) provides the loading control (lanes 1 and 2). SWP1 and SWP2 primers are located downstream and upstream of the first intron of the *SWP* gene, respectively (see C), excluding genomic contamination of the reverse transcribed RNA samples, which would have led to an 1 kb amplification product as shown in lane 6. (**C**) Schematic representation of the T-DNA insertion site in the *swp* mutant line. The T-DNA caused a 6 bp deletion at the predicted transcription start site of the *SWP* gene (arrow, WT transcription start). In *swp*, initiation of transcription may occur at upstream functional sites existing within the T-DNA and could be driven by the cauliflower mosaic virus promoter (35S) as suggested by the high expression level detected in *swp*. The sequence of the region of fusion between the *SWP* mRNA and T-DNA left border (LB) is given. In the T-DNA LB sequence (underlined), several putative start codons (bold letters) are detected that could compete with the wild-type *SWP* start codon, potentially leading to transcriptional attenuation in *swp* mutant, as suggested by the recessive nature of the *swp* mutation. bar, basta (ammonium glufosinate) herbicide resistance gene; tnos, nos gene terminator.

germination, *SWP* was strongly expressed in young leaf primordia. This expression was maintained in developing leaves. A weak signal, sometimes just above the detection level, was also visible at the vegetative shoot apical meristem (Figure 8C). A stronger signal was observed throughout the inflorescence meristem. Expression was further upregulated in the young floral primordia (Figure 8D). During flower development, *SWP* was expressed in floral organ primordia, but absent or only weakly expressed in mature organs (Figure 8D and F). The expression was maintained in meiocytes and the tapetum in anthers (Figure 8E) and later in the ovules (Figure 8F).

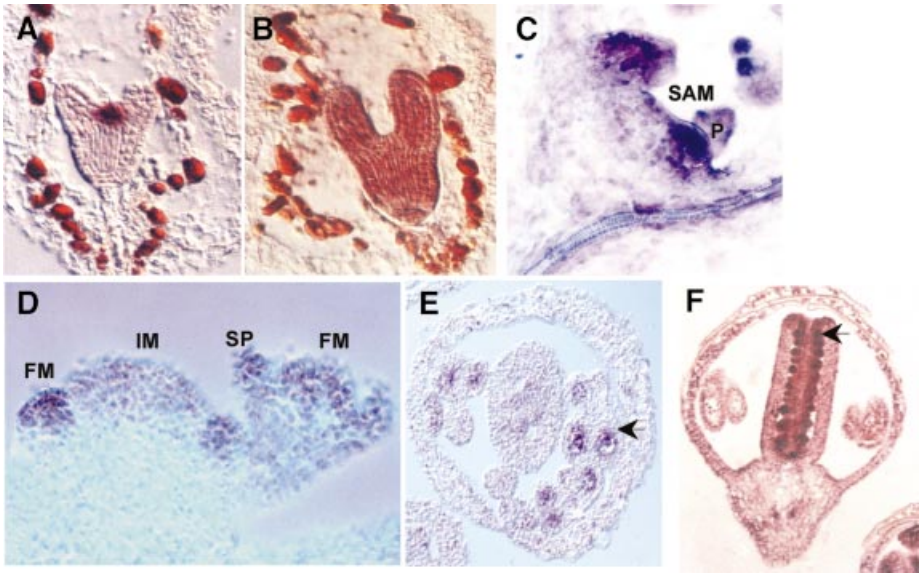

Fig. 8. *SWP* RNA expression pattern. *SWP* mRNA was detected using *in situ* hybridization. (**A**) A STM antisense control probe showing SAM-specific expression in a young torpedo stage embryo. (**B**) A torpedo stage embryo in the same experiment showing *SWP* mRNA expression in all cells. (**C**) In the 8-day-old seedling apex, strong *SWP* expression was detected in the primordia (P) and weakly in the SAM. (**D**) In the inflorescence meristem (IM) *SWP* is also detected, but more mRNA was present in the lateral floral meristems (FM), and in young organ primordia of developing flowers (SP: sepal primordia). (**E**) *SWP* mRNA was also present in meiocytes and tapetum within the anthers (arrowhead). (**F**) The expression was maintained in ovules (arrowhead) within the gynoecium in later stages of flower development.

The specificity of the expression pattern was confirmed using two different regions of the *SWP* gene as probes that gave identical results. In addition, sense probes gave no signal (data not shown). Additional expression analysis by northern blot analysis showed that *SWP* is also expressed in roots, stems and in cell suspension (data not shown).

Overexpression of SWP

To gain further insight into *SWP* function, we overexpressed the gene using a constitutive promoter. For this purpose, a genomic sequence was put under the control of the 35S CaMV promoter. A total of 26 lines with a similar heritable, dominant phenotype were obtained. Of these transgenics, three (lines 145 and 31 in L*er* and line 2.9 in WS) were analysed further. Although the effect was variable, plants from these lines were smaller, the size of all aerial organs being severely reduced in a majority of the plants (Figure 9A, B and H). However, the overall structure of the organs was normal and all three transgenic lines were fertile, although seed production was severely reduced. The dwarved phenotype became gradually visible from ~2 weeks onwards. For all three lines, the observed phenotype was associated with an overproduction of *SWP* mRNA (Figure 9C). The similar reduction in organ size observed both in plants overpressing *SWP* and *swp* loss of function mutants was initially difficult to explain. We therefore looked at the cellular phenotype of the overexpressers. Microscopy of fully expanded leaves of plants with a strong overexpresser phenotype grown in the glasshouse revealed an important effect on epidermal cell size (Figure 9D–G). Epidermal pavement cells with an almost normal size were intermingled with groups of much smaller cells. This suggested that the arrest of cell division in the transgenic leaves was less synchronous than in the wild type. To extend the SEM results, the first two fully expanded leaves of five plants grown *in vitro* were harvested and fixed. Leaf size and cell area were subsequently measured as described above for the kinematic analysis. The quantitative analysis confirmed that the mean cell size in the leaves of the transgenic lines was reduced (Figure 9I). Nevertheless, the range of cell sizes observed in the transgenic lines was comparable with the wild type (Figure 10A). The smaller cells tended to be clustered (Figures 9D–G and 10). Defining, arbitrarily, a small cell as a cell with a surface of <500 μm^2, we found that 16% of these cells were present in clusters of five cells or more. In the wild type, this percentage was below 1%. This suggested that in the overexpressing line, cells locally continued to divide, while their neighbours had already stopped, resulting in groups of small cells adjacent to bigger ones. Due to the variability of the phenotype, it was difficult to perform a kinematic analysis, but together the results showed that the moment of cell cycle arrest in the overexpressers was less synchronized when compared with the wild type. This effect was very localized, suggesting a cell autonomous effect of the transgene. We next examined the effects on total cell numbers. Although this effect was variable from leaf to leaf, we found that the total number of cells per leaf was increased by ~54% (Figure 9J). We conclude that in the leaves of overexpressers, cell cycle arrest was more asynchronous. In addition, the final cell number was increased, while cell size was reduced, which is the opposite of the *swp* loss of function phenotype.

Discussion

During a screen for mutants perturbed in meristem function and organ initiation (Laufs *et al.*, 1998a), we identified a subclass of lines that also showed alterations in cell number. We are using these lines as tools to study both the control and developmental significance of cell

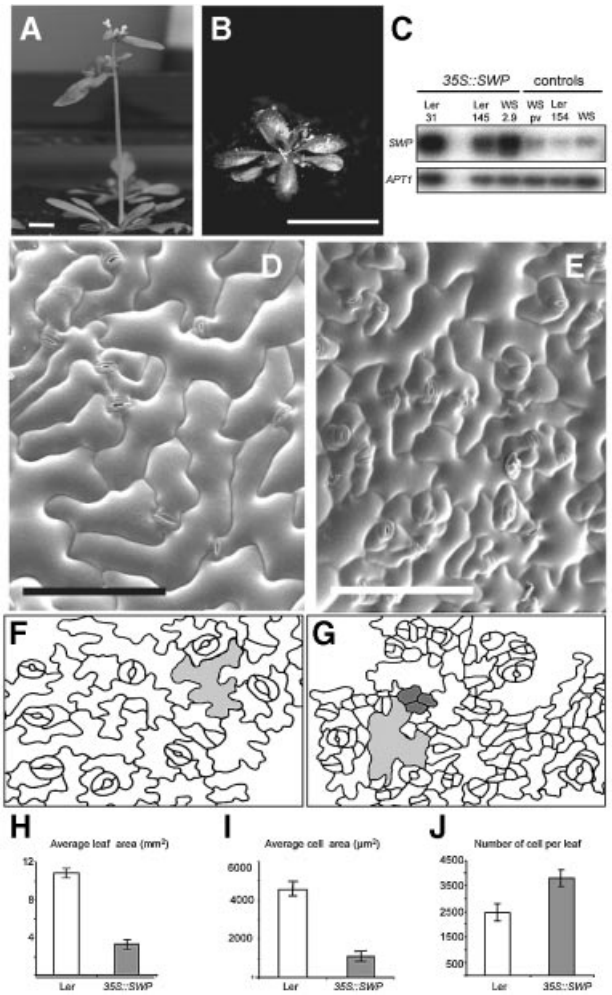

Fig. 9. Overexpression of *SWP*. (**A**) Control plant (ecotype L*er*) grown in soil. (**B**) *35S::SWP* primary transformant (line 145; ecotype L*er*) grown in soil. (**C**) Over-accumulation of *SWP* transcript in 21-day-old 35S::*SWP* plants, line 31 (L*er*), 145 (L*er*) and 2.9 (WS) using semi-quantitative PCR. Controls: *SWP* levels in a line transformed with the empty binary plasmid (pv, WS) in a line that did not present a phenotype (L*er* 154) and in the wild type (WS). APT1 was used as a loading control. (**D–G**) Epidermis of mature first rosette leaves of 3-week-old control (D and F) and *35S::SWP* (line 145) (E and G) plants was visualized using SEM (adaxial epidermis; D and E) or tubu drawings (abaxial epidermis; F and G). Average leaf area was measured (**H**), average cell area (**I**) was estimated using the tubu drawings as described for the kinematic analysis of leaf growth, then average cell number per leaf (**J**) was calculated. Scale bars: 0.5 cm in (A) and (B); 125 µM in (D) and (E).

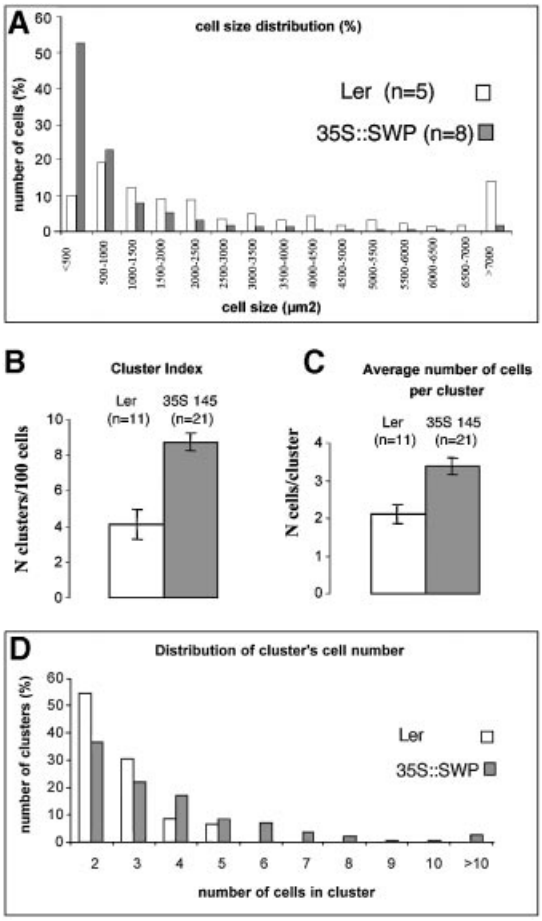

Fig. 10. Clustering of cells on leaves overexpressing *SWP*. (**A**) Cell area distribution in wild-type (L*er*) and 35S::SWP leaves. Cell area was measured on tubu images of the abaxial epidermis of the first leaves of 28-day-old wild-type (292 cells measured on five independent leaves) and 35S::SWP plants (line 145, 1077 cells measured, eight independent leaves). Guard cells were excluded from the measurements. The number of cells in each size class was scored. (**B**) 'Cluster' index. The clustering of cells was determined in the leaves of 21 35S::*SWP* leaves and 11 wild-type leaves. Per leaf, at least a surface of 100 cells was analysed. A cluster of cells was defined as a group of two or more small cells with an area <500 µm^2. The cluster index is defined as the number of cell clusters in a population of 100 cells. (**C**) Average number of cells per cluster. The number of cells was scored in each cluster of wild-type (46 clusters in 11 leaves) and overexpressing leaves (298 clusters in 21 leaves). (**D**) Distribution of cell number per cluster.

proliferation in plants, two topics that are still poorly understood.

The control of cell numbers in leaves

After recruitment to the leaf primordia, the cells go through a stage of mitotic activity. In *Arabidopsis*, this period is followed by several rounds of endoreduplication, after which the cells grow further without cycling until they finally differentiate. Although very little is currently known concerning the mechanisms involved, cell numbers in a plant organ could, in theory, be regulated at different levels: (i) the amount of cells initially recruited to the primordium; (ii) the timing or window of cell division (start/arrest of cell proliferation); and (iii) the cell proliferation rate. Genetic and transgenic approaches have shown that these variables are not necessarily coupled. Overexpression of the cyclin-dependent kinase (CDK) inhibitors KRP1 and KRP2, for example, reduces the maximum proliferation rate in young leaves, without affecting the timing of cell cycle arrest and differentiation (Wang *et al*., 2000; De Veylder *et al*., 2001). Here we show, using both loss and gain of function analysis, that *SWP*, in contrast, perturbs the timing or window of cell division, but leaves maximum cell division rates (cell cycle duration) unchanged.

Another well-characterized gene involved in defining the window of cell proliferation in the primordium is *AINTEGUMENTA* (*ANT*) in *Arabidopsis*. Inactivation and overexpression of this transcription factor reduces and increases the total cell number in lateral organs, respectively, without affecting proliferation rates (Mizukami and

Fisher, 2000). In all eukaryotes, the G_1 phase seems to be a major checkpoint in the decision to stop or to continue cell proliferation. In plants, like in animals, the initiation of cell division probably involves the inactivation of the retinoblastoma (RB) protein by the appropriate CDKs and D-cyclins. This would involve two transcription factors, E2F and Dpa, which, also in plants, are involved in the activation of cell cycle genes and in the maintenance of proliferative capacity (De Veylder *et al*., 2002). During cell differentiation, the opposite process is thought to occur, i.e. a reactivation of RB blocks the cells in G_1, inducing cell differentiation (e.g. Ach *et al*., 1997). In the case of ANT, a direct link was made with D-cyclin expression as ANT overexpression causes an ectopic activation of CYCD3, suggesting that the window of cell proliferation could be influenced in this way. Work is now under way to see whether the early arrest of cell division in *swp* is also caused by the abnormal expression of cell cycle regulators.

Cell numbers, compensation mechanisms and organ size control

As indicated earlier, in *Drosophila* wings, a reduction or increase in the amount of cells does not dramatically alter the final size of the organs, as changes in cell size make up for the modifications in cell numbers. To explain this compensation, it has been proposed that organ size might be controlled by 'total mass checkpoint' mechanisms, which operate at the level of whole organs (reviewed in Potter and Xu, 2001). These mechanisms couple cell proliferation and cell growth, enabling cell size to compensate for the lack or excess of cells and vice versa, thus guaranteeing a certain size of the body or organ. Although not much is known about the processes involved, several mutations potentially disrupting such a total mass checkpoint have been identified in animals, involving insulin and nutrient signalling pathways (Oldham *et al*., 2000; Weinkove and Leevers, 2000). The idea is in fact reminiscent of the so-called organismal theory advocated by Kaplan and Hagemann (1991), who proposed that development is not regulated at the level of individual cells, but rather at the level of entire compartments or even whole organisms. Along the same line, Day and Lawrence (2000) suggested the existence of hormone or growth factor gradients covering entire organs. In their scenario, cells continue to grow until a certain steepness of the gradient is obtained, or until a certain distance from the source of growth factor is reached.

In plants, compensatory mechanisms also exist, which are active during the rapid, post-mitotic expansion of the differentiating cells. Thus, mutations in *ant* or overexpression of KRPs cause reduced cell numbers, which are subsequently masked by an increase in the final cell size. However, it must be noted that in these examples, compensation is not always complete. KRP overexpression leads to a 10-fold reduction in cell numbers, which is only compensated partially by a 6-fold increase in cell size. The overall result is a reduction of the total leaf volume by ~35% (De Veylder *et al*., 2001). Although it could be argued that in KRP overexpressers the limits of compensation are reached, this is not very likely for *swp* mutants, where leaf size is reduced up to 90% and cell size only increases by 30%, far less than the 600% increase reported for KRP overexpressers. *In vitro*, this is even more dramatically illustrated, as cells in the *swp* mutant and wild type have comparable sizes. Mutation of SWP therefore clearly affects the capacity of the leaves to compensate for a reduction in cell number and could affect the definition of the proposed total mass checkpoint in leaves. In this respect, the results obtained from plants overexpressing *SWP* are of interest. Since both cell size and leaf size are reduced, it appears that the mechanisms coordinating post-mitotic cell expansion are perturbed again. This phenotype could be explained in several ways. First, the transgene could again interfere with a process operating at the level of the whole leaf. However, it is also possible that the cellular responses themselves are inhibited. The small cells in these lines do not have the typical puzzle shape of their bigger sisters and look more like the meristematic-type cells observed in very young primordia. This cellular phenotype is reminiscent of what is observed in plants overexpressing meristematic genes such as *KNAT1* and *KNAT2* (Chuck *et al*., 1996; Pautot *et al*., 2001). Therefore, it could be that the smaller epidermal cells in 35S::*SWP* are in another differentiation state and are not competent to react properly to the signals controlling post-mitotic cell expansion. Similar observations were also made for *Arabidopsis* plants overexpressing E2F and Dpa, which showed an increase in cell number, but a reduction in overall organ shape (De Veylder *et al*., 2002).

We also noted that the compensation for reduced cell number was not systematically observed in all organs. This was particularly striking for the floral organs, where petals showed a 2- to 3-fold reduction in cell number, which was not compensated by extra cell growth. In KRP overexpressers and *ant* or *swp* mutants, the compensatory mechanisms operate at the level of post-mitotic cell expansion. However, *swp* also points to another earlier moment where compensation could be actively regulated: the endoreduplicative phase which precedes and accompanies the rapid post-mitotic cell expansion in the *Arabidopsis* leaf. Interestingly, *SWP* clearly affects the switch to endoreduplication, as cells exit earlier from mitosis and a significant amount goes through one extra round of endoreduplication. The exact role of endoreduplication has not been determined, but it could represent an alternative to cell division by increasing the growth potential of a cell population (Traas *et al*., 1998) and a compensation by endoreduplication would anticipate the growth defects due to the lack of cells. In this context, it is interesting to note that flowers and floral organs do not show extensive endoreduplication (Galbraith *et al*., 1991), and that we did not observe compensation for reduced numbers in petals.

Molecular basis of SWP function: a role in transcriptional regulation?

The *swp* mutant produces oversized chimeric mRNAs containing T-DNA sequences fused to their 5′ end, which are probably under the control of the T-DNA 35S CaMV promoter. Although we cannot exclude the possibility that some protein is produced, our results nevertheless suggest that the mutation causes a loss of function since *swp* is a recessive mutation, which can be complemented by a single copy of the wild-type gene. In addition, a weak *swp*

phenotype was observed in *swp* transgenic plants partially complemented by the wild-type gene. This indicates that the *swp* allele we have studied is at least an intermediary loss of function mutation, which affects cell numbers and SAM function throughout plant development.

The predicted SWP protein has nuclear localization signals and shows significant homologies with metazoan and yeast Med150/RGR1 proteins in its N-terminal region. Biochemical studies have shown that the large Med150/RGR1 proteins belong to regulatory units called Mediator complexes, which function in transcriptional control. It has been proposed that these complexes are recruited by nuclear receptors in the presence of ligands such as thyroid hormone, glucocorticoids (Ito *et al*., 1999) or vitamin D3 (Rachez *et al*., 1998). Consistent with these results, SWP contains three LXXLL signature motifs identified previously as nuclear receptor interaction domains (Rachez *et al*., 1998; Yuan *et al*., 1998; Fondell *et al*., 1999). The Mediator complexes would then act as transcriptional co-activators by recruiting in turn, for instance, proteins with histone acetyltransferase activity, creating a more accessible chromatin structure for the RNA polymerase II pre-initiation complex (PIC) (Yang *et al*., 1999; Ito and Roeder, 2001). Distinct modular Mediator complexes may coexist in the nucleus, allowing transmission of various signals from different classes of activators to the PIC. Information concerning the physiological roles of Mediator complexes remains rare (Li *et al*., 1995; Jiang *et al*., 1998; Gu *et al*., 1999; Lee *et al*., 1999; for a review, see Rachez and Freedman, 2001). In humans, nuclear hormone receptors interacting with the Mediator complex are involved in the control of cell growth and differentiation, development and several physiological processes (for a review, see Ito and Roeder, 2001).

The highest homologies to the SWP protein are found in the *Drosophila* sequence. A small domain of strong similarity in the C-terminal part of the sequence could indicate a functional importance of this domain for the activity of the proteins. So far, no *Drosophila* mutants for this gene have been isolated. However, mutants in two different subunits of the *Drosophila* Mediator complex, dMed240/dTRAP240 and dMed80/dTRAP80, have been described. Both mutations are recessive lethal and show synergistic interactions between each other and with the homeotic *Scr* locus, suggesting that this homeodomain protein activity is modulated by the Mediator complex during development (Boube *et al*., 2000).

Concluding remarks

Although our analysis has focused on cell number in the developing leaves, the *SWP* gene probably has other roles. First, the gene is also expressed, albeit weakly, in the SAM. Accordingly, the SAM is severely disorganized as shown by a patchy *STM* expression of the cells in the meristematic region and the extension of the cell population expressing *WUS*, a gene involved in meristem maintenance. To our knowledge, such a meristematic phenotype has not been described previously. At this stage, it is not possible to determine how the meristem phenotype is linked to the leaf phenotype. However, the gene is most strongly expressed in the young leaves and the leaf phenotype appears before the meristem becomes disorganized. Therefore, the meristem defect could at least partially be triggered by the perturbations arising in the young leaves. Another aspect of the mutation, not addressed here in detail, is the altered leaf shape. Histological analysis indicated that the mutant leaves usually had a normal tissue polarity, although the most severely affected and smallest leaves tend to be finger-like and radial symmetric. Indeed, the apparent loss of symmetry appeared to be directly correlated with the number of cells in the mutant leaves (data not shown) and it would be interesting to analyse this potential link between cell proliferation and organ shape.

The proposed molecular function of the gene, its expression pattern and mutant phenotype would suggest a very broad function of *SWP* in the plant. Nevertheless, we did not observe any obvious embryonic or root phenotypes. This can be interpreted in different ways. If a partially functional protein is produced in the mutant, the phenotype would mainly become visible at stages where the requirement for *SWP* would be particularly critical. Alternatively, if no functional *SWP* is formed, proteins with redundant functions could be active. In any case, our results reveal a particular requirement for *SWP* at the shoot apex in the regulation of the window of cell proliferation.

Materials and methods

Plant growth conditions and mutant isolation

Plants were grown *in vitro* as described by Santoni *et al*. (1994). Nutrient medium as described by Estelle and Sommerville (1987) with 1% sucrose was used. After sowing, plates were left for 2 days at 4°C to synchronize germination. For the analysis of mature leaves, plants were grown in soil in a greenhouse under regulated conditions as described by Laufs *et al*. (1998b). The *swp* mutant was identified *in vitro* at the seedling stage in a T-DNA insertion mutagenesis screen (WS ecotype; Bechtold *et al*., 1993; Bouchez *et al*., 1993).

SWP gene cloning

The *swp* phenotype is genetically linked to the kanamycin resistance locus of a single T-DNA insertion. Genomic DNA flanking the right border of the T-DNA was cloned by plasmid rescue (Bouchez *et al*., 1996), while genomic DNA flanking the left border was recovered by inverse PCR (Lindsey and Topping, 1996). Routine DNA manipulations were performed according to Sambrook *et al*. (1989). Genomic fragments flanking both right and left borders were used to screen an *Arabidopsis* Columbia genomic phage library (EEC-bridge *Arabidopsis* DNA Stock Center). Positive clones fell into two partially overlapping groups. One clone of each group was chosen for subcloning into pBluescript II SK (–) (Stratagene) and sequenced. EST H10G5T7 representing a partial 3′end 3081 bp cDNA was provided by H.Höfte. 5′ RACE was performed using a kit (Gibco-BRL) according to the manufacturer's protocol to amplify a 2466 bp fragment. For the complementation test, a 9700 bp wild-type genomic DNA *Apa*I fragment from a phage clone subcloned into pBluescript II SK (–) was used, corresponding to nucleotides 70635–79908 of the F7O18 BAC sequence (accession No. AC011437.6), putatively comprising the entire *SWP* gene with 1755 bp upstream of the predicted start codon, and 1000 bp after the cDNA 3′ end. The fragment was converted to blunt-end using T4-DNA polymerase exonuclease activity, *Bam*HI digested, cloned into the *Sma*I–*Bam*HI sites of the pCambia 1300 plant transformation vector (Cambia LTD, Camberra, Australia) and electroporated into *Agrobacterium tumefasciens* strain C58C1 (pMP90; Konz and Schell, 1986). Plants heterozygous for the *swp* mutation were transformed using the floral dipping method (Clough and Bent, 1998).

SWP mRNA expression in swp mutant

For RNA blot analysis, poly(A)$^+$ RNA was isolated using a classical phenol extraction protocol and Dynabeads purification kit (Dynal AS, Oslo, Norway). Approximately 4 μg of poly(A)$^+$ RNA were probed with an antisense RNA probe synthesized by T3 polymerase and radiolabelled with an *in vitro* transcription kit (Promega, Madison, WI), using a 600 bp

*Xba*I–*Hin*dIII SWP cDNA fragment cloned into pBluescript II SK (–) as a template. This probe corresponded to the 3′ end of SWP cDNA, including the 3′ untranslated region and its specificity was verified by Southern blot analysis. Prehybridization, hybridization, washes and detection were performed as described by Vernoux *et al*. (2000a). As an equal loading control (data not shown), the blot was hybridized with a PCR-generated probe detecting EIF1aA4 translation elongation factor mRNA (Liboz *et al*., 1990; accession No. X16432). For RT–PCR analysis, RNA was isolated using the RNeasy kit (Qiagen). The RNA was treated with DNase and first-strand cDNA synthesis was performed on 1 µg of total RNA with the superscriptRT-II (Gibco-BRL) and anchored oligo d(T)20 according to the manufacturer's intructions. Ten per cent of the first-strand reaction was used for PCR amplification with SWP primers swpUp (5′-ATGGCGGAATTAGGGCAACAGACGGTGG-3′) and swpLow (5′-ATGCCGTCTTGTCACTTCAAGTTTAAT-3′) and T-DNA pGKB5 vector (Bouchez *et al*., 1993) primer LB1 (5′-CTACAAATTGCC-TTTTCTTATCGAC-3′).

Construction of 35S::SWP lines

The *35S::SWP* construct was made by inserting a 7 kb genomic fragment, encompassing the *SWP* gene from translation initiation codon to 100 bp after the 3′ end of the cDNA, between the 35S CaMV promoter and the nopaline synthase polyadenylation sequence into the plant expression vector pMD1 (kindly provided by M.Pastuglia). To obtain this construction, a first genomic fragment, corresponding to the 1.4 kb 5′ end, was generated by PCR amplification using the primer swpUp (see above) modified to introduce a *Bam*HI site upstream of ATG initiation codon and the primer swp1.2Low (5′-CCTCTCCTTCTTGGTTCGT-CGGTG-3′) with Extend High Fidelity DNA polymerase (Boehringer Mannheim). After cloning into the *Bam*HI–*Kpn*I sites of pBluescript II SK (–), the fragment was sequenced. This 1.4 kb *Bam*HI–*Kpn*I fragment was inserted together with a 5.6 kb *Kpn*I–*Xho*I 3′ end genomic fragment from a phage clone into the *Bam*HI and *Xho*I sites of the pMD1 vector. The construct was introduced into *A.tumefasciens* strain C58C1 (pMP90; Konz and Schell, 1986) by electroporation. Wild-type plants [ecotypes Landsberg *Erecta* (L*er*) or WS] were transformed using the floral dipping method (Clough and Bent, 1998). *SWP* mRNA levels in *35S::SWP* lines were estimated using semi-quantitative RT–PCR as described in Nesi *et al*. (2000). To determine whether the same amounts of RNA had been sampled from the different lines, we used two control primers, APT1-Up (5′-ATGCCCCAGGACATCGTGATTTCAT-3′) and APT1-Low (5′-TTGGCGGCACCCTTAGCTGGATCA-3′), designed from exons 1 and 2, respectively, of the *APT1* gene (accession No. X58640; Moffatt *et al*., 1992). For mRNA detection of the *SWP* gene, the specific primers designed from exons 6 and 7 were swp5,8Up (5′-GAAGGC-CGCTCTCTTGAATT-3′) and swp6,5Low (5′-CCTAACTGATAC-ACAGTAAG-3′), respectively.

Kinematic analysis of leaf development

The kinematic analysis of *swp* and wild-type (ecotype WS) leaf growth was performed as described by De Veylder *et al*. (2001) with the following modifications: (i) *in vitro* growth conditions as described above were used; (ii) for each time point, one leaf from the first leaf pair from at least five independent plants was analysed, and from day 6 to day 10, the measurements were performed twice using independently grown sets of plants; (iii) for wild-type leaves, from day 9 to day 20, cell density and stomatal index were determined from scanned drawing tubus images of at least 30 cells of the abaxial epidermis located 25 and 75% of the distance between the tip and base of the blade, halfway between the mid-rib and leaf margin. In the youngest primordia, from day 6 to day 8, a single group of cells from the tip to the base of the primordium, halfway between the mid-rib and leaf margin, was drawn. This method has been validated as representative of cell and stomata numbers of the whole leaf at different stages. Due to the very reduced *swp* leaf size from day 6 to day 16, a single group of cells, as described for wild-type young primordia, was drawn. For later stages (days 18 and 20), *swp* cells were drawn in the same way as in wild-type leaves; and (iv) stomatal index reported in our experiment is the fraction of stomata in the total population of epidermal cells (instead of the fraction of guard cells reported in the original method).

Confocal microscopy and SEM

For analysis of cell proliferation rate in living primordia, one cotyledon of the young seedling was dissected under binoculars to allow visualization of the shoot apex. Seedlings were placed in glass bottom observation plates, the seedling root being embedded in *in vitro* growth nutrient medium as described above, to allow continuous growth of the plants. Seedlings were stained with 0.1 µg/ml FM1-43 (Molecular Probes, Leiden, The Netherlands) dissolved in low melting point agarose, and viewed with an inverted Leica TCSNT confocal laser scanning microscope (Leica, Heidelberg, Germany) equipped with an argon/krypton laser (Omnichrome, Chino, CA), using a ×40 long working distance water immersion apochromat objective (Leica). FM1-43 fluorescence was monitored with a 505–530 nm band pass emission filter (488 nm excitation line). Between each series of image recordings, the observation plates were placed vertically in a growth chamber. Reconstructions of serial sections in order to visualize epidermal cells only, and primordia area measurements were made with Optimas 5.2 image analysis software (Bioscan, Imasys, Suresne, France). The individual cell divisions were scored on the reconstruction image series as the formation of a new cell wall. The surface of mature organs was visualized using low-temperature SEM as described by Traas *et al*. (1995).

Alternatively, the mitotic index or nuclear DNA content was determined on fixed material stained for DNA content with propidium iodide as described by Laufs *et al*. (1998a).

Histological analysis and in situ hybridization

Histological sections and *in situ* hybridizations were carried out as described by Vernoux *et al*. (2000b). Full-length cDNA *STM* and *WUS* probes were generous gifts from Dr K.Barton (University of Wisconsin-Madison, WI) and Dr T.Laux (University of Tübingen, Germany), respectively. To generate *SWP*-specific sense and antisense RNA probes, a 1.3 kb *Hin*dIII fragment corresponding to the *SWP* cDNA 5′ end or a 1.6 kb *Cla*I fragment corresponding to the 3′ end of the cDNA, including untranslated regions, was cloned into pBluescript II SK (–) and used as template for *in vitro* transcription and labelling using digoxigenin (DIG-UTP, Boehringer Mannheim) according to the manufacturer's instructions.

Flow cytometric analysis

After removal of the leaf petioles, leaf blades were chopped with a razor blade directly in DAPI (0.5 µg/ml)-containing staining buffer (Galbraith *et al*., 1983). After filtration over a 30 µm mesh, the nuclei were analysed on a flow cytometer (EPICS V; Coulter).

Acknowledgements

We are grateful to Tom Beeckman for the help with the tubu microscope, and to Spencer Brown and colleagues for flow cytometric analysis. We thank Patrick Laufs, Olivier Hamant, Veronique Pautot and Trine Juul for critical reading of the manuscript. This work was supported by two EEC programmes: ECCO (to K.B.) and REGIA (to J.T.). C.J. was supported by an EMBO long-term fellowship, and D.A. by the French MRT.

References

Ach,R.A., Durfee,T., Miller,A.B., Taranto,P., Hanley-Bowdoin,L., Zambryski,P. and Gruissem,W. (1997) *RRB1* and *RRB2* encode maize retinoblastoma-related proteins that interact with a plant D-type cyclin and geminivirus replication protein. *Mol. Cell. Biol.*, **17**, 5077–5086.

Altschul,S.F., Madden,T.L., Schäffer,A.A., Zhang,J., Zhang,Z., Miller,W. and Lipman,D.J. (1997) Gapped BLAST and PSI-BLAST: a new generation of protein database search programs. *Nucleic Acids Res.*, **25**, 3389–3402.

Bechtold,N., Ellis,J. and Pelletier,G. (1993) *In planta Agrobacterium* mediated gene transfer by infiltration of adult *Arabdopsis thaliana* plants. *C. R. Acad. Sci. Life Sci.*, **316**, 1194–1199.

Boube,M., Faucher,C., Joulia,L., Cribbs,D.L. and Bourbon,H.M. (2000) *Drosophila* homologs of transcriptional mediator complex subunits are required for adult cell and segment identity specification. *Genes Dev.*, **14**, 2906–2917.

Bouchez,D., Camillieri,C. and Caboche,M. (1993) A binary vector based on Basta resistance for *in planta* transformation of *Arabidopsis thaliana*. *C. R. Acad. Sci. Life Sci.*, **316**, 1188–1193.

Bouchez,D., Vittorioso,P., Courtial,B. and Camilleri,C. (1996) Kanamycin rescue: a simple technique for the recovery of T-DNA flanking sequences. *Plant Mol. Biol. Rep.*, **14**, 115–123.

Chuck,G., Lincoln,C. and Hake,S. (1996) *KNAT1* induces lobed leaves with ectopic meristems when overexpressed in *Arabidopsis*. *Plant Cell*, **8**, 1277–1289.

Clough,S.J. and Bent, A.F. (1998) Floral dip: a simplified method for

Agrobacterium-mediated transformation of *Arabdopsis thaliana*. *Plant J.*, **16**, 735–743.
Conlon,I. and Raff,M. (1999) Size control in animal development. *Cell*, **96**, 235–244.
Day,S.J. and Lawrence,P.A. (2000) Measuring dimensions: the regulation of size and shape. *Development*, **127**, 2977–2987.
De Veylder,L. *et al*. (2001) Functional analysis of cyclin-dependent kinase inhibitors of *Arabidopsis*. *Plant Cell*, **13**, 1–15.
De Veylder,L. *et al*. (2002) Control of proliferation, endoreduplication and differentiation by *Arabidopsis* E2Fa-DPa transcription factor. *EMBO J.*, **21**, 1360–1368.
Estelle,M.A. and Somerville,C.R. (1987) Auxin-resistant mutants of *Arabidopsis thaliana* with an altered morphology. *Mol. Gen. Genet.*, **206**, 200–206.
Fondell,J.D., Guermah,M., Malik,S. and Roeder,R.G. (1999) Thyroid hormone receptor-associated proteins and general positive co-factors mediate thyroid hormone receptor function in the absence of the TATA box-binding protein-associated factors of TFIID. *Proc. Natl Acad. Sci. USA*, **96**, 1959–1964.
Galbraith,D.W., Harkins,K.R., Maddox,J.R., Ayres,N.M., Sharma,D.P. and Firoozabady,E. (1983) Rapid flow cytometric analysis of the cell cycle in intact plant tissues. *Science*, **220**, 1049–1051.
Galbraith,D., Harkins,K. and Knapp,S. (1991) Systemic endoploidy in *Arabidopsis thaliana*. *Plant Physiol.*, **96**, 985–989.
Gu,W., Malik,S., Ito,M., Yuan,C.X., Fondell,J.D., Zhang,X., Martinez,E., Qin,J. and Roeder,R.G. (1999) A novel human SRB/MED-containing cofactor complex, SMCC, involved in transcription regulation. *Mol. Cell*, **3**, 97–108.
Hemerly,A., Engler,J.D.A., Bergounioux,C., Van Montagu,M., Engler,G., Inze,D. and Ferreira,P. (1995) Dominant negative mutants of the Cdc2 kinase uncouple cell division from iterative plant development. *EMBO J.*, **14**, 3925–3936.
Ito,M. and Roeder,R.G. (2001) The TRAP/SMCC/Mediator complex and thyroid hormone receptor function. *Trends Endocrinol. Metab.*, **12**, 127–134.
Ito,M. *et al*. (1999) Identity between TRAP and SMCC complexes indicates novel pathways for the function of nuclear receptors and diverse mammalian activators. *Mol. Cell*, **3**, 361–370.
Jiang,Y.W.,Veschambre,P.,Erdjument-Bromage,H.,Tempst,P.,Conaway, J.W., Conaway,R.C. and Kornberg,R.D. (1998) Mammalian mediator of transcriptional regulation and its possible role as en end-point of signal transduction pathways. *Proc. Natl Acad. Sci. USA*, **95**, 8538–8543.
Kaplan,D.R. and Hagemann,W. (1991) The relationship of cell and organism in vascular plants: are cells the building blocks of plant form? *Bioscience*, **41**, 693–703.
Kim,J., Harter,K. and Theologis,A. (1997) Protein–protein interactions among the Aux/IAA proteins. *Proc. Natl Acad. Sci. USA*, **94**, 11786–11791.
Konz,C. and Schell,J. (1986) The promoter of TL-DNA gene controls the tissue specific expression of chaemeric genes carried by a novel type *Agrobacterium tumefaciens*. *Mol. Gen. Genet.*, **204**, 383–396.
Laufs,P., Dockx,J., Kronenberger,J. and Traas,J. (1998a) *MGOUN1* and *MGOUN2*: two genes required for primordium initiation at the shoot apical and floral meristems in *Arabidopsis thaliana*. *Development*, **125**, 1253–1260.
Laufs,P., Grandjean,O., Jonak,C., Kieu,K. and Traas,J. (1998b) Cellular parameters of the shoot apical meristem in *Arabidopsis*. *Plant Cell*, **10**, 1375–1390.
Lee,D., Kim,S. and Lis,J.T. (1999) Different upstream transcriptional activators have distinct coactivator requirements. *Genes Dev.*, **13**, 2934–2939.
Li,Y., Bjorklund,S., Jiang,Y.W., Kim,Y.J., Lane,W., Stillman,D.J. and Kornberg,R.D. (1995) Yeast global transcriptional regulators Sin4 and Rgr1 are components of mediator complex/RNA polymerase II holoenzyme. *Proc. Natl Acad. Sci. USA*, **92**, 10864–10868.
Liboz,T., Bardet,C., Le Van Thai,A., Axelos,M. and Lescure,B. (1990) The four members of the gene family encoding the *Arabdopsis thaliana* translation elongation factor EF-1α are actively transcribed. *Plant Mol. Biol.*, **14**, 107–110.
Lindsey,K. and Topping,J.F. (1996) T-DNA-mediated insertional mutagenesis. In Foster,G.D. and Twell,D. (eds), *Plant Gene Isolation: Principles and Practice*. John Wiley & Sons, New York, NY, pp. 275–300.
Long,J.A., Moan,E.I., Medford,J.I. and Barton,M.K. (1996) A member of the *KNOTTED* class of homeodomain proteins encoded by the *STM* gene of *Arabidopsis*. *Nature*, **379**, 66–69.
Mayer,K.F., Schoof,H., Haecker,A., Lenhard,M., Jurgens,G. and Laux,T. (1998) Role of *WUSCHEL* in regulating stem cell fate in the *Arabidopsis* shoot meristem. *Cell*, **95**, 805–815.
Mizukami,Y. and Fischer,R.L. (2000) Plant organ size control: *AINTEGUMENTA* regulates growth and cell numbers during organogenesis. *Proc. Natl Acad. Sci. USA*, **97**, 942–947.
Moffatt,B.A., McWhinnie,E.A., Burkhart,W.E., Pasternak,J.J. and Rothstein,S.J. (1992) A complete cDNA for adenine phosphoribosyltransferase from *Arabidopsis thaliana*. *Plant Mol. Biol.*, **18**, 653–662.
Nesi,N., Debeaujon,I., Jond,C., Pelletier,G., Caboche,M. and Lepiniec,L. (2000) The *TT8* gene encodes a basic helix–loop–helix domain protein required for expression of DFR and BAN genes in *Arabidopsis* siliques. *Plant Cell*, **12**, 1863–1878.
Oldham,S., Bohni,R., Stocker,H., Brogiolo,W. and Hafen,E. (2000) Genetic control of size in *Drosophila*. *Philos. Trans. R. Soc. Lond. B Biol. Sci.*, **355**, 945–952.
Pautot,V., Dockx,J., Hamant,O., Kronenberger,J., Grandjean,O., Jublot,D. and Traas,J. (2001) *KNAT2*: evidence for a link between *Knotted*-like genes and carpel development. *Plant Cell*, **13**, 1–17.
Potter,C.J. and Xu,T. (2001) Mechanisms of size control. *Curr. Opin. Genet. Dev.*, **11**, 279–286.
Rachez,C. and Freedman,L. (2001) Mediator complexes and transcription. *Curr. Opin. Cell Biol.*, **13**, 274–280.
Rachez,C., Suldan,Z., Ward,J., Chang,C.P., Burakov,D., Erdjument-Bromage,H., Tempst,P. and Freedman,L.P. (1998) A novel protein complex that interacts with the vitamin D3 receptor in a ligand-dependent manner and enhances VDR transactivation in a cell-free system. *Genes Dev.*, **12**, 1787–1800.
Raff,M.C. (1996) Size control: the regulation of cell numbers in animal development. *Cell*, **86**, 173–175.
Raikhel,N. (1992) Nuclear targeting in plants. *Plant Physiol.*, **100**, 1627–1632.
Sambrook,J., Fritsch,E.F. and Maniatis,T. (1989) *Molecular Cloning: A Laboratory Manual*. Cold Spring Harbor Laboratory Press, Cold Spring Harbor, NY.
Santoni,V., Bellini,C. and Caboche,M. (1994) Use of two-dimensional protein-pattern analysis for the characterization of *Arabidopsis thaliana* mutants. *Planta*, **192**, 557–566.
Traas,J. and Doonan,J. (2001) Cellular basis of shoot apical meristem development. *Int. Rev. Cytol.*, **208**, 161–206.
Traas,J., Bellini,C., Nacry,P., Kronenberger,J., Bouchez,D. and Caboche,M. (1995) Normal differentiation patterns in plant lacking microtubular preprophase bands. *Nature*, **375**, 676–677.
Traas,J., Hülskamp,M., Gendreau,E. and Höfte,H. (1998) Endoreduplication and development: rule without dividing? *Curr. Opin. Plant Biol.*, **1**, 498–503.
Van Lijsebettens,M. and Clarke,J. (1998) Leaf development in *Arabidopsis*. *Plant Physiol. Biochem.*, **36**, 47–60.
Vernoux,T. *et al*. (2000a) The *ROOT MERISTEMLESS1/CADMIUM SENSITIVE2* gene defines a glutathione-dependent pathway involved in initiation and maintenance of cell division during postembryonic root development. *Plant Cell*, **12**, 97–110.
Vernoux,T., Kronenberger,J., Grandjean,O., Laufs,P. and Traas,J. (2000b) *PIN-FORMED 1* regulates cell fate at the periphery of the shoot apical meristem. *Development*, **127**, 5157–5165.
Vernoux,T., Autran,D. and Traas,J. (2000c) Developmental control of cell division patterns in the shoot apex. *Plant Mol. Biol.*, **43**, 569–581.
Wang,H., Zhou,Y., Gilmer,S., Whitwill,S. and Fowke,C.L. (2000) Expression of the plant cyclin-dependent kinase inhibitor ICK1 affects cell division, plant growth and morphology. *Plant J.*, **24**, 613–623.
Weinkove,D. and Leevers,S.J. (2000) The genetic control of organ growth: insights from *Drosophila*. *Curr. Opin. Genet. Dev.*, **10**, 75–80.
Yang,Z., Hong,S.H. and Privalsky,M.L. (1999) Transcriptional anti-repression. Thyroid hormone receptor β-2 recruits SMRT corepressor but interferes with subsequent assembly of a functional corepressor complex. *J. Biol. Chem.*, **274**, 37131–37138.
Yuan,C.X., Ito,M., Fondell,J.D., Fu,Z.Y. and Roeder,R.G. (1998) The TRAP220 component of thyroid hormone receptor-associated protein (TRAP) coactivator complex interacts directly with nuclear receptors in a ligand-dependent fashion. *Proc. Natl Acad. Sci. USA*, **95**, 7939–7944.

Received January 10, 2002; revised June 17, 2002; accepted September 26, 2002